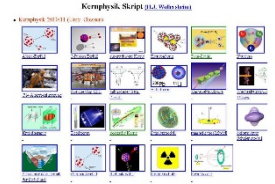


Outline: Projectile fragmentation

Lecturer: Hans-Jürgen Wollersheim

e-mail: h.j.wollersheim@gsi.de

web-page: <https://web-docs.gsi.de/~wolle/> and click on



1. fragmentation cross section
2. nuclear reaction rates
3. in-flight separation of **R**adioactive **I**on **B**eams
4. fragment separator at GSI and FAIR
5. identification of **RIB**s

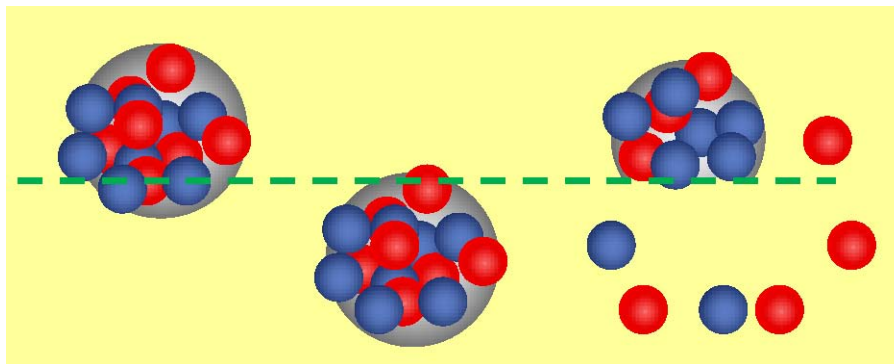
Projectile fragmentation reaction

Discovery

at Bevalac @ LBL (Lawrence Berkeley Laboratory)

D.E. Greiner et al., Phys.Rev. Lett. 35 (1975) 152

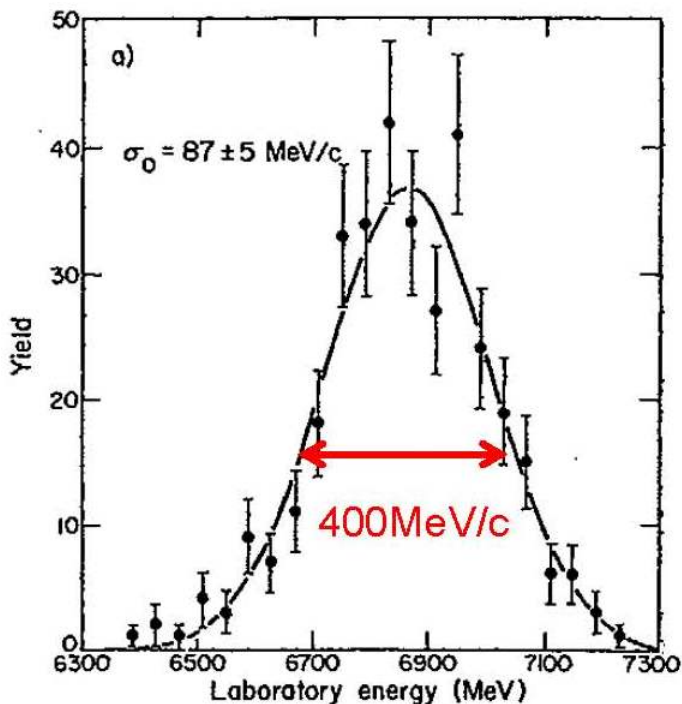
^{12}C , ^{16}O (2.1 AGeV) + Target (Be, C, Al, Cu, Ag, Pb)



- Several fragments are produced in reactions
- Velocity of fragments is almost the same as that of the beam
- Momentum distribution is narrow, and has no significant correlation with target mass and beam energies

Projectile fragmentation reaction

Momentum distribution of fragments (example ^{34}S fragments from $^{40}\text{Ar} + \text{C}$ @ 213 A MeV)

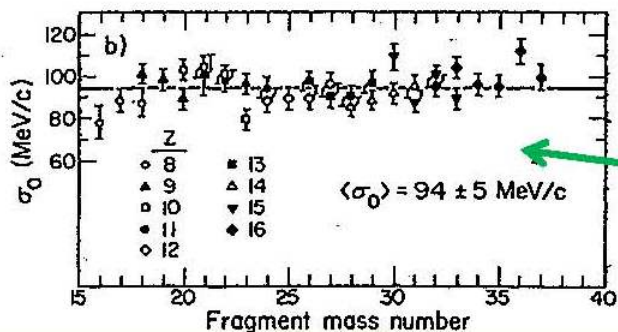


^{34}S fragments: 400 MeV/c narrow
 ^{40}Ar beam: 26600 MeV/c

Momentum distribution of fragments are represented by a simple formula based on the Goldhaber model

$$\sigma = \sigma_0 \cdot \sqrt{\frac{F \cdot (A - F)}{(A - 1)}}$$

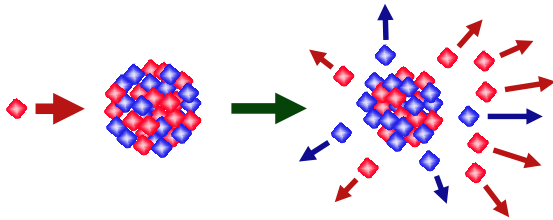
A: beam mass number
 F: fragment mass number



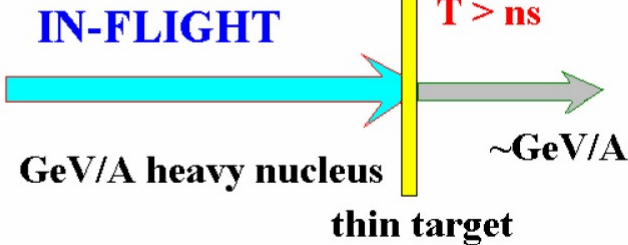
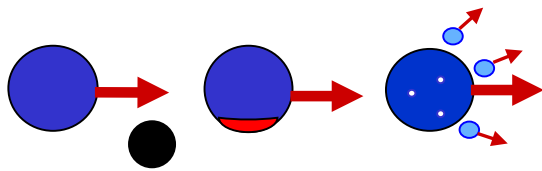
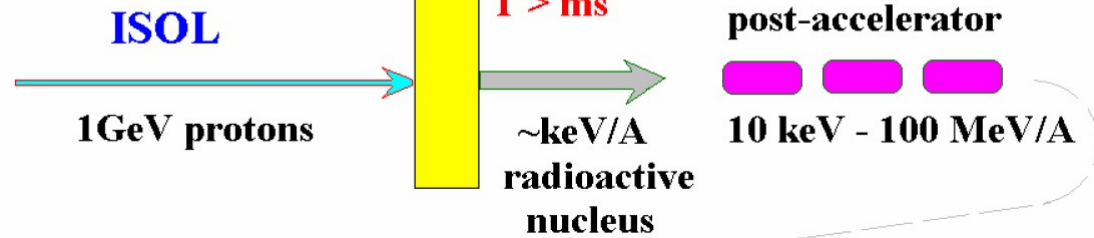
$\sigma_0 = 90$ MeV/c

Spallation & projectile fragmentation reactions route to exotic nuclei

Spallation



thick target +
ion source



Fragmentation

ISOL = Isotope Separator On Line

High-energy proton-induced nuclear reactions

Some early high-energy proton accelerators:

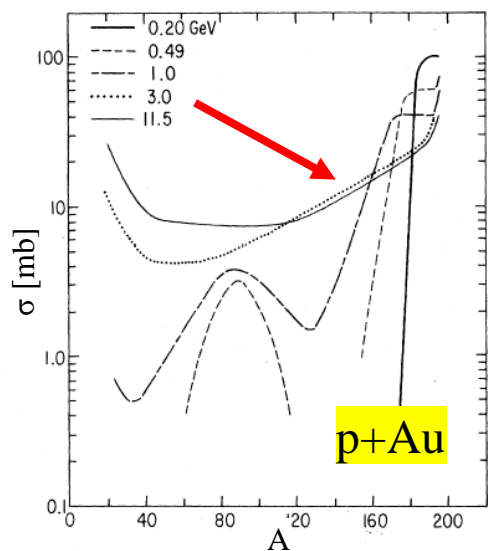
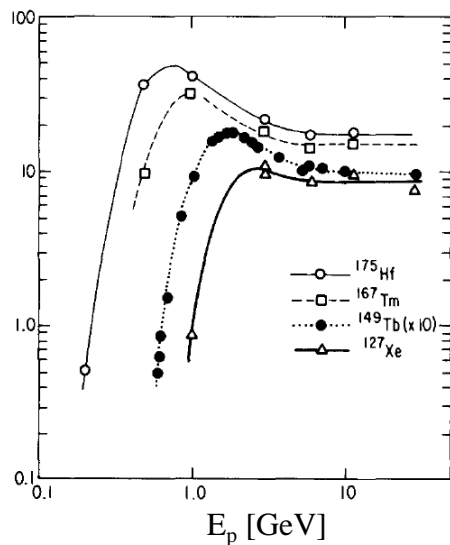
Facility	Energy	from year
Bevatron (Berkeley)	6 GeV	1954.....
AGS (Brookhaven)	11 GeV	1960.....
Fermilab (Chicago)	>300 GeV	1967.....

They were also used to bombard various stable target materials.

These targets were analyzed with radiochemical methods,
i.e. γ -spectroscopy with or without chemical separators

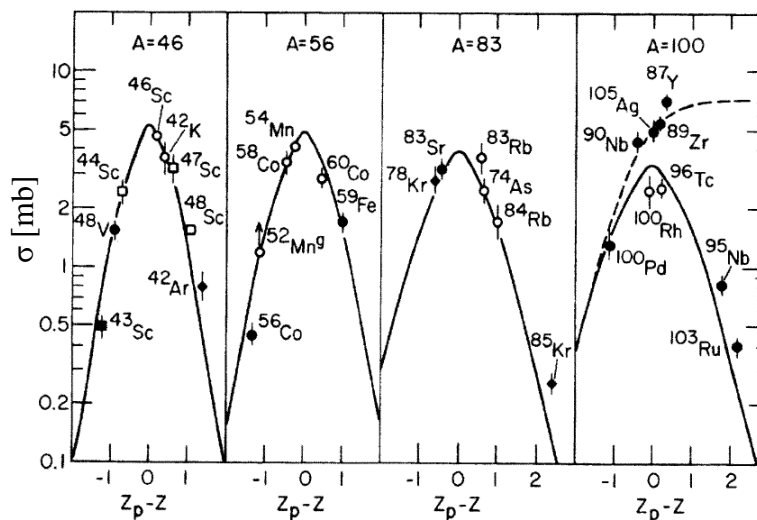
 **Production cross sections and (some) kinematics for suitable radioactive isotopes**

High-energy proton-induced nuclear reactions



Important findings:

- ❖ Energy-independence of cross sections
- ❖ Bell-shaped Z-distribution for constant A



- ❖ Mass yields: exponential slope

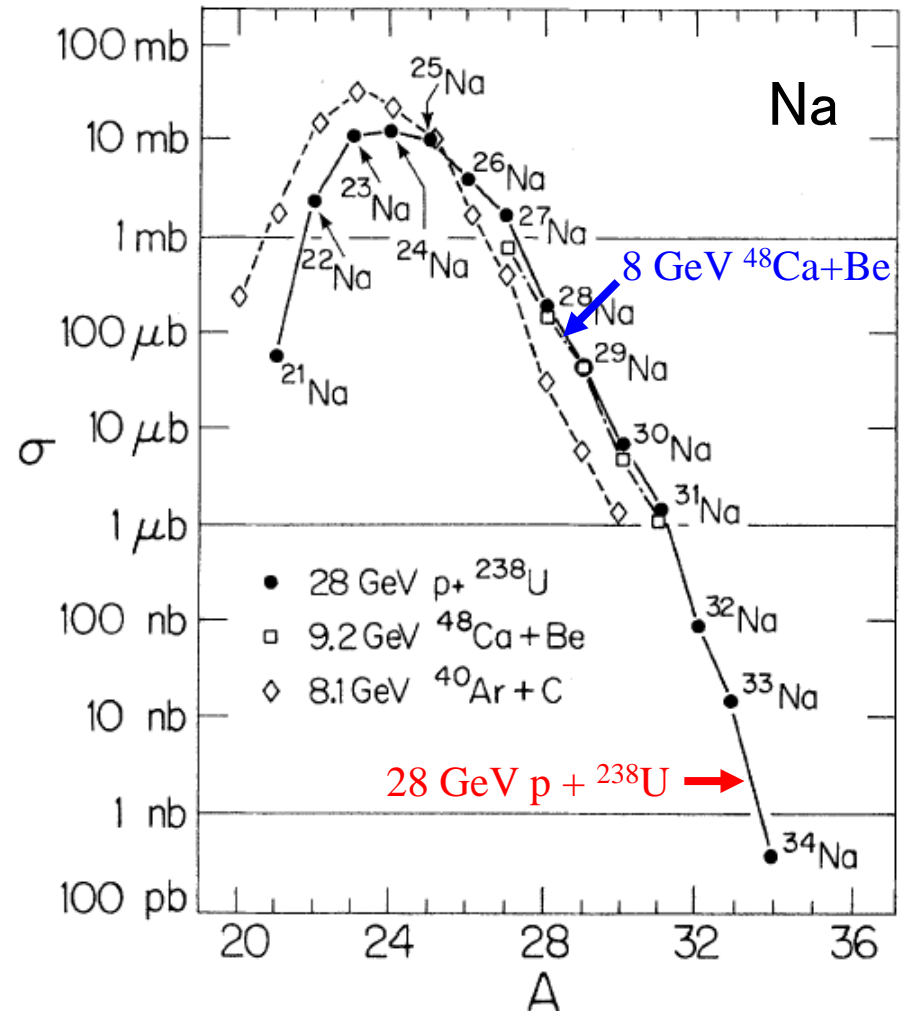
Proton- versus heavy-ion induced reactions

Proton- and heavy-ion induced reactions give very similar isotope distribution:

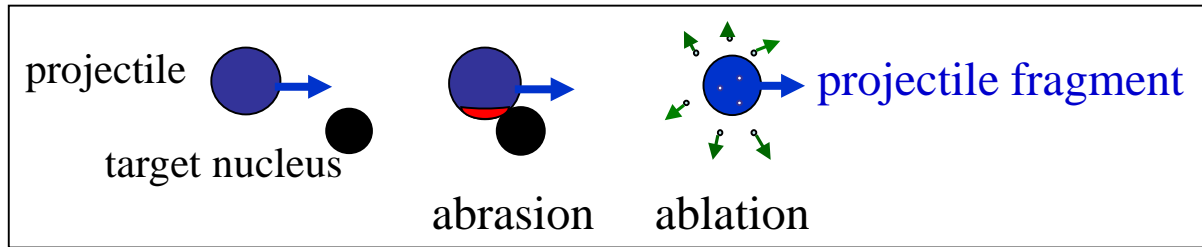
Target fragmentation: $\text{GeV } p + A_{\text{target}} \rightarrow A$

Projectile fragmentation: $\text{GeV}/u A_{\text{proj}} + p \rightarrow A$

are equivalent



Projectile fragmentation reactions



At GeV energies nucleons can be regarded as a classical particles

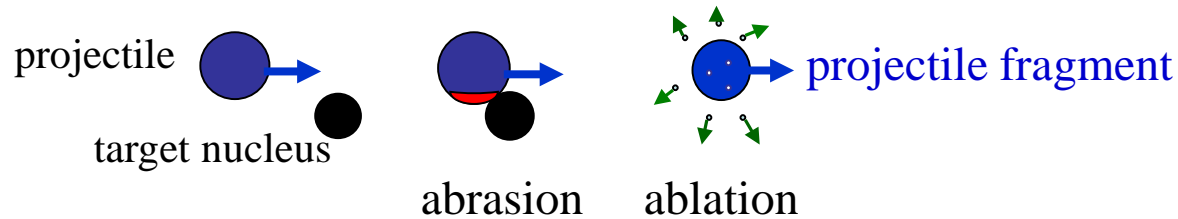
- Nucleon-nucleon collisions can be treated classically using measured free nucleon-nucleon cross sections (intra-nuclear cascade).
- In these collisions very *little transfer momentum* is exchanged.
- After the cascade the residual nucleus is *highly excited*.
- Heavy-ion projectiles can be treated as a bag of individual nucleons.

Physical models: Two-step approach

Step 1: **Abrasion** models or **Intranuclear-cascade** models (10^{-23} s)

Step 2: **Ablation**: nucleons evaporated (final fragment 10^{-19} s)

Projectile fragmentation reactions abrasion-ablation model



Empirical parameterization of fragmentation cross section:

EPAX v.3 K. Sümmerer, Phys. Rev. C86 (2012) 014601

<http://web-docs.gsi.de/~weick/epax/>

EPAX V3, Empirical parametrization of fragmentation cross sections
by Klaus Sümmerer, March 2012

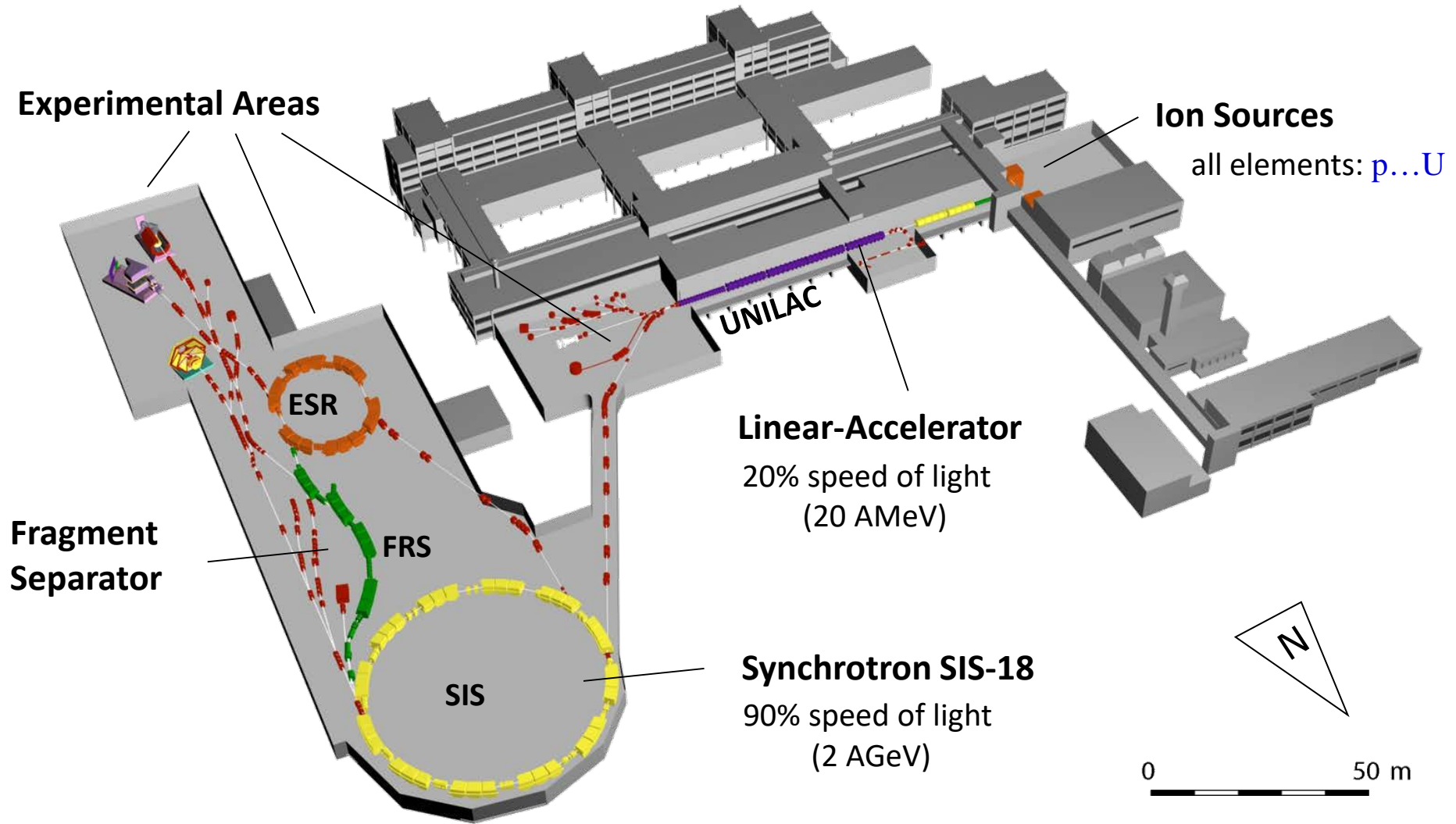
projectile:		target:		fragment:	
Ap	Zp	At	Zt	Af	Zf
<input type="text" value="58"/>	<input type="text" value="28"/>	--> on <input type="text" value="9"/>	<input type="text" value="4"/>	--> to <input type="text" value="48"/>	<input type="text" value="28"/>

EPAX V3, Empirical parametrization of fragmentation cross sections

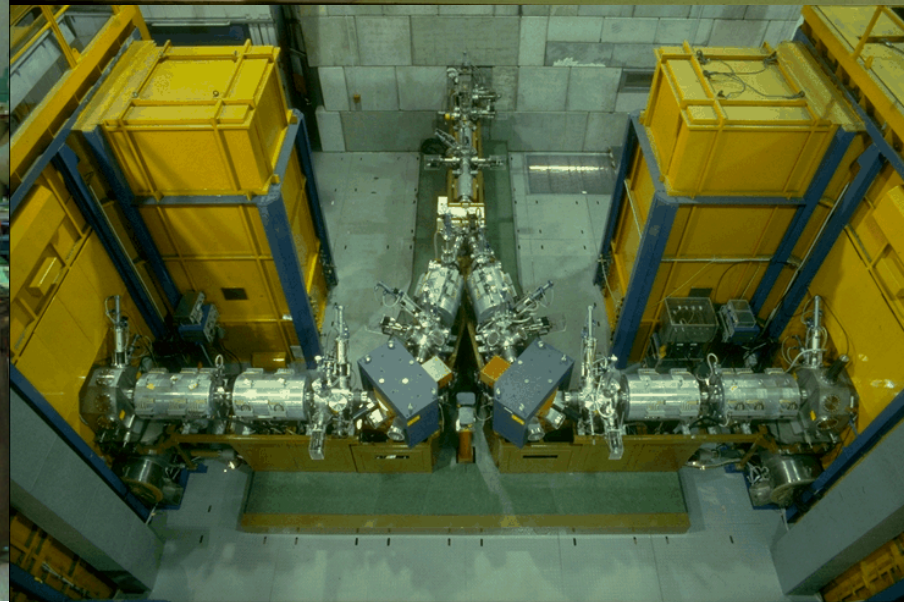
EPAX Version 3.1
by Klaus Sümmerer, 15.03.2012

Fragmentation cross section !!:
projectile Ap=58.000000 Zp=28.000000
on target At=9.000000 Zt=4.000000
to produce Af=48.000000 Zf=28.000000
sigma = 1.407530e-14 b

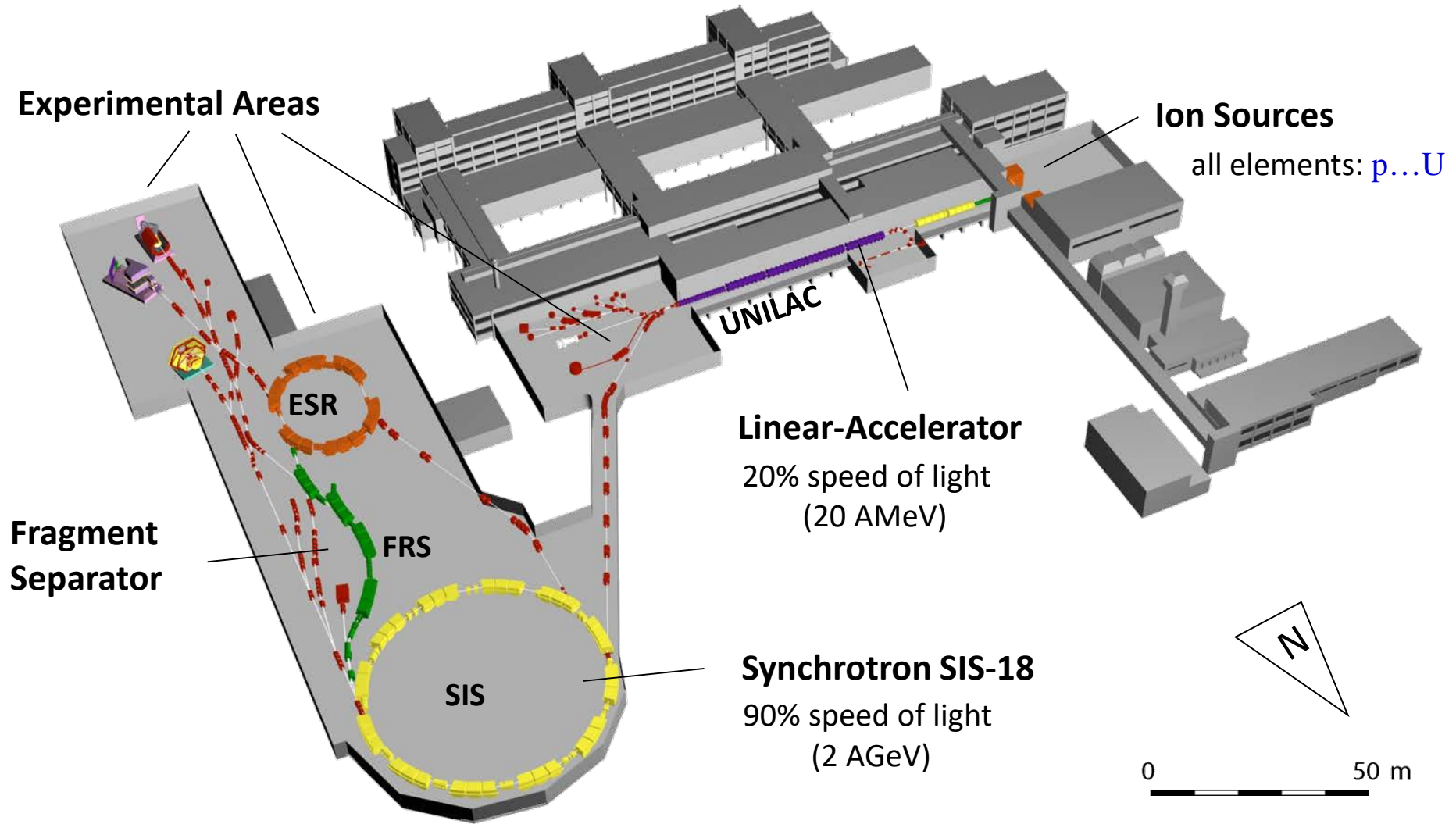
The accelerator facility at GSI



UNILAC accelerator



The accelerator facility at GSI

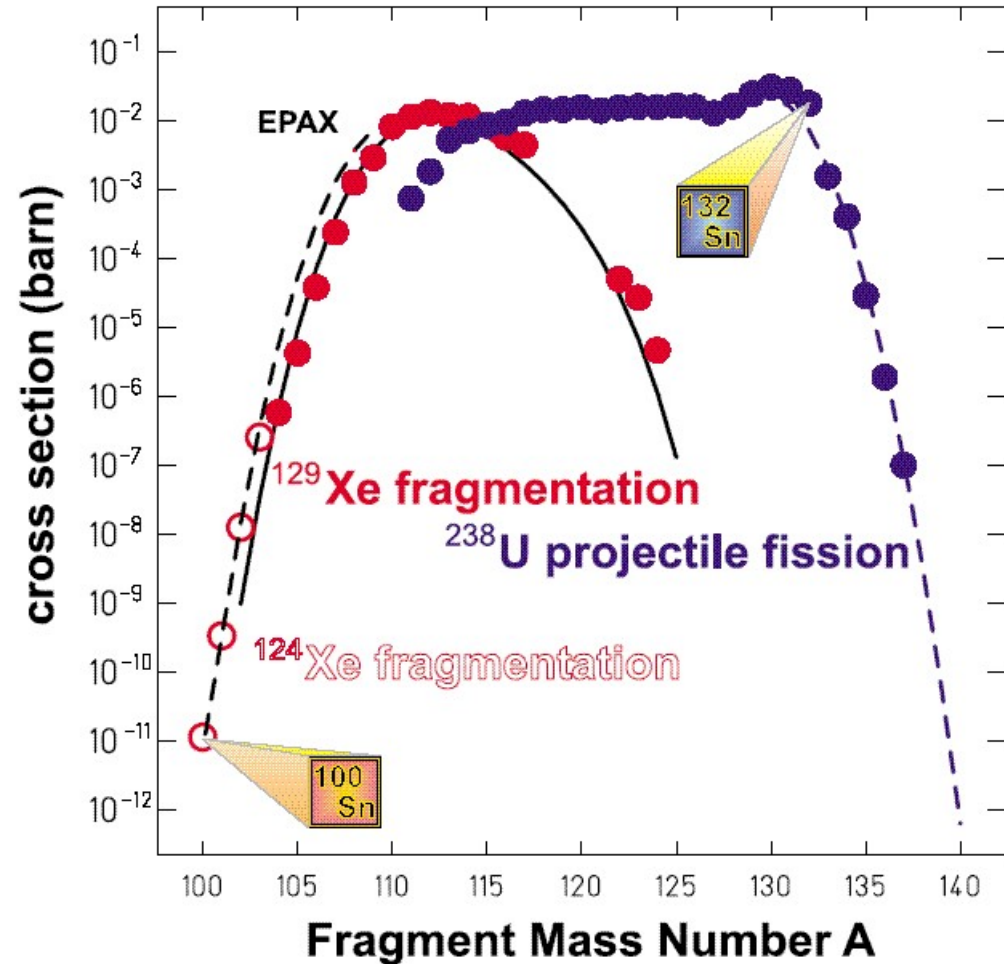
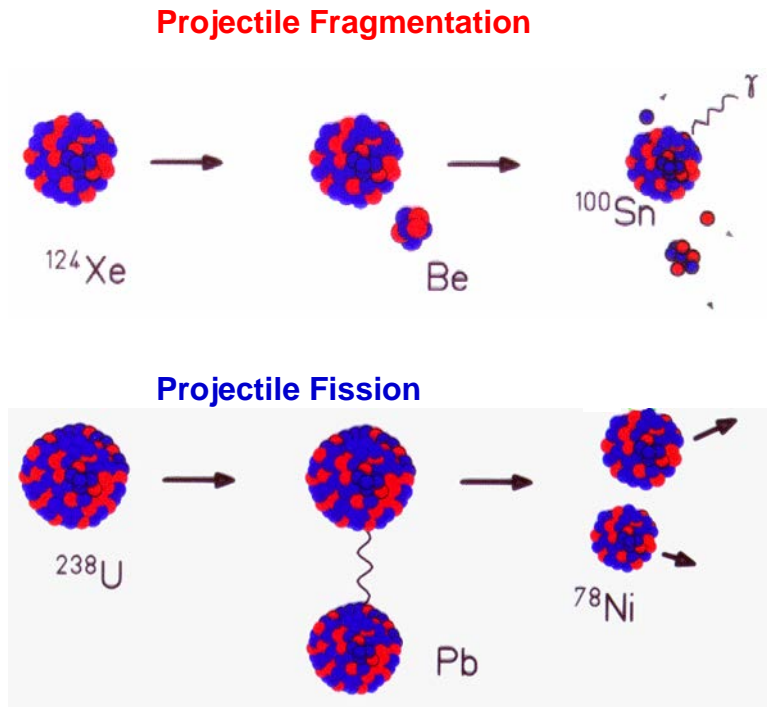




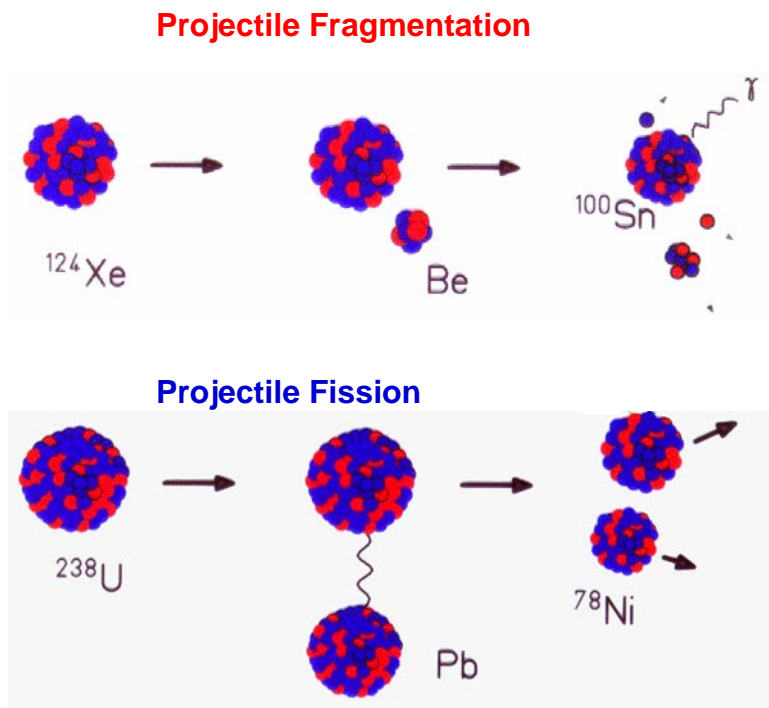
Where do we do the experiments?



Projectile fragmentation reactions



Secondary beam intensities at S4



transmission SIS-FRS: 70%

primary Xe-beam intensity: $2.5 \cdot 10^9 [\text{s}^{-1}]$

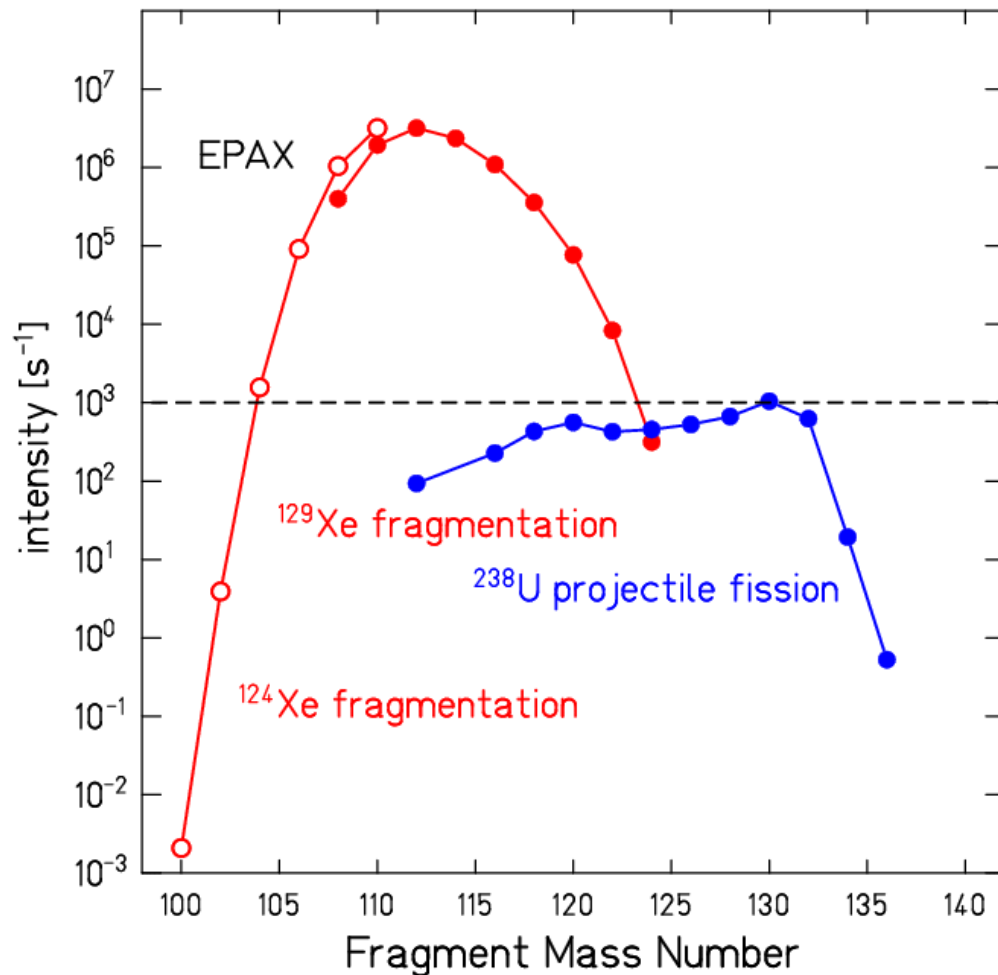
Be-target thickness: 4g/cm^2

transmission through FRS: 60%

primary U-beam intensity: $10^9 [\text{s}^{-1}]$

Pb-target thickness: 1g/cm^2

transmission through FRS: 2%

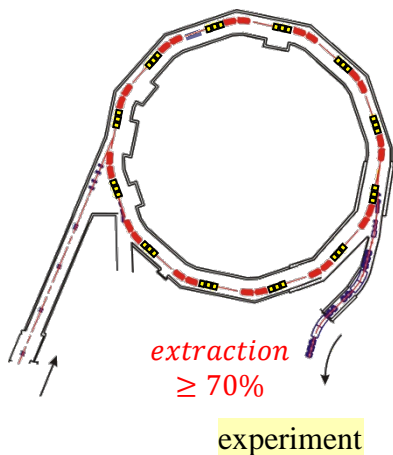
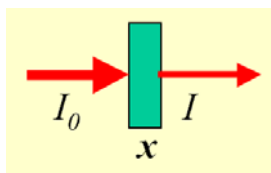
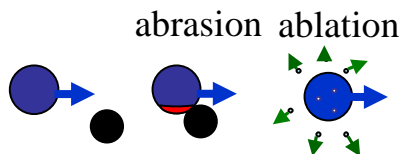


Nuclear reaction rate

➤ nuclear reaction rate [s^{-1}] = luminosity [$\text{atoms cm}^{-2} s^{-1}$] * σ_f [cm^2]

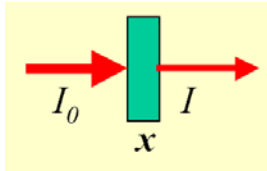
➤ σ_f [cm^2] for projectile fragmentation + fission

➤ luminosity [$\text{atoms cm}^{-2} s^{-1}$] = projectiles [s^{-1}] * target nuclei [cm^{-2}]



Ion	SIS-18 (2008)	SIS-100 (expected)	
$^{20}\text{Ne}^{10+}$	$2 \cdot 10^{11}$	$^{20}\text{Ne}^{7+}$	$1.6 \cdot 10^{12}$
$^{40}\text{Ar}^{18+}$	$1 \cdot 10^{11}$	$^{40}\text{Ar}^{10+}$	$1.4 \cdot 10^{12}$
$^{58}\text{Ni}^{26+}$	$9 \cdot 10^{10}$	$^{58}\text{Ni}^{14+}$	$1.3 \cdot 10^{12}$
$^{84}\text{Kr}^{34+}$	$8 \cdot 10^{10}$	$^{84}\text{Kr}^{17+}$	$1.2 \cdot 10^{12}$
$^{132}\text{Xe}^{48+}$	$7 \cdot 10^{10}$	$^{132}\text{Xe}^{22+}$	$1.3 \cdot 10^{12}$
$^{197}\text{Au}^{65+}$	$5 \cdot 10^{10}$	$^{197}\text{Au}^{25+}$	$1.2 \cdot 10^{12}$
$^{238}\text{U}^{73+}$	$1.6 \cdot 10^{10}$	$^{238}\text{U}^{92+}$	$1.4 \cdot 10^{10}$
$^{238}\text{U}^{28+}$	$1.4 \cdot 10^{10}$	$^{238}\text{U}^{28+}$	$5.0 \cdot 10^{11}$

Nuclear reaction rate



density ρ

Primary reaction rate:

$$\phi_f [s^{-1}] \cong \phi_p [s^{-1}] \cdot \frac{x [g/cm^2] \cdot 6.02 \cdot 10^{23}}{A_t [g]} \cdot \sigma_f [cm^2] \quad (\text{thin target})$$

Example: ^{238}U ($10^9 s^{-1}$) on ^{208}Pb ($x=1 g/cm^2$) \rightarrow ^{132}Sn ($\sigma_f=15.4 mb$) reaction rate: 44571 [s^{-1}]

Example: ^{124}Xe ($10^9 s^{-1}$) on ^9Be ($x=1 g/cm^2$) \rightarrow ^{104}Sn ($\sigma_f=5.6 \mu b$) reaction rate: 375 [s^{-1}]

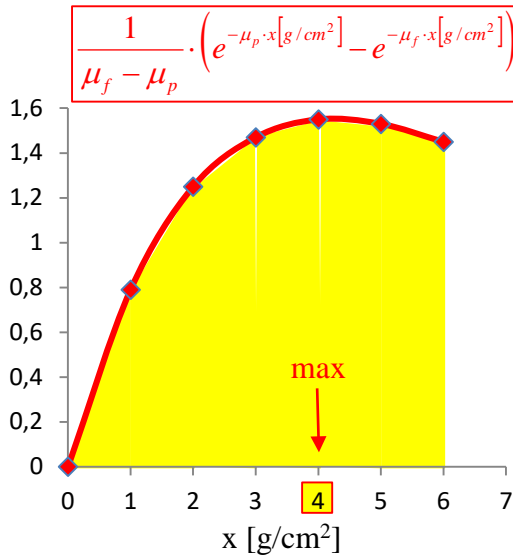
The **optimum thickness** of the production target is limited by the loss of fragments due to secondary reactions

Primary + secondary reaction rate:

$$\phi_f [s^{-1}] = \phi_p [s^{-1}] \cdot \frac{6.02 \cdot 10^{23} \cdot \sigma_f [cm^2]}{A_t [g]} \cdot \frac{1}{\mu_f - \mu_p} \cdot \left(e^{-\mu_p \cdot x [g/cm^2]} - e^{-\mu_f \cdot x [g/cm^2]} \right)$$

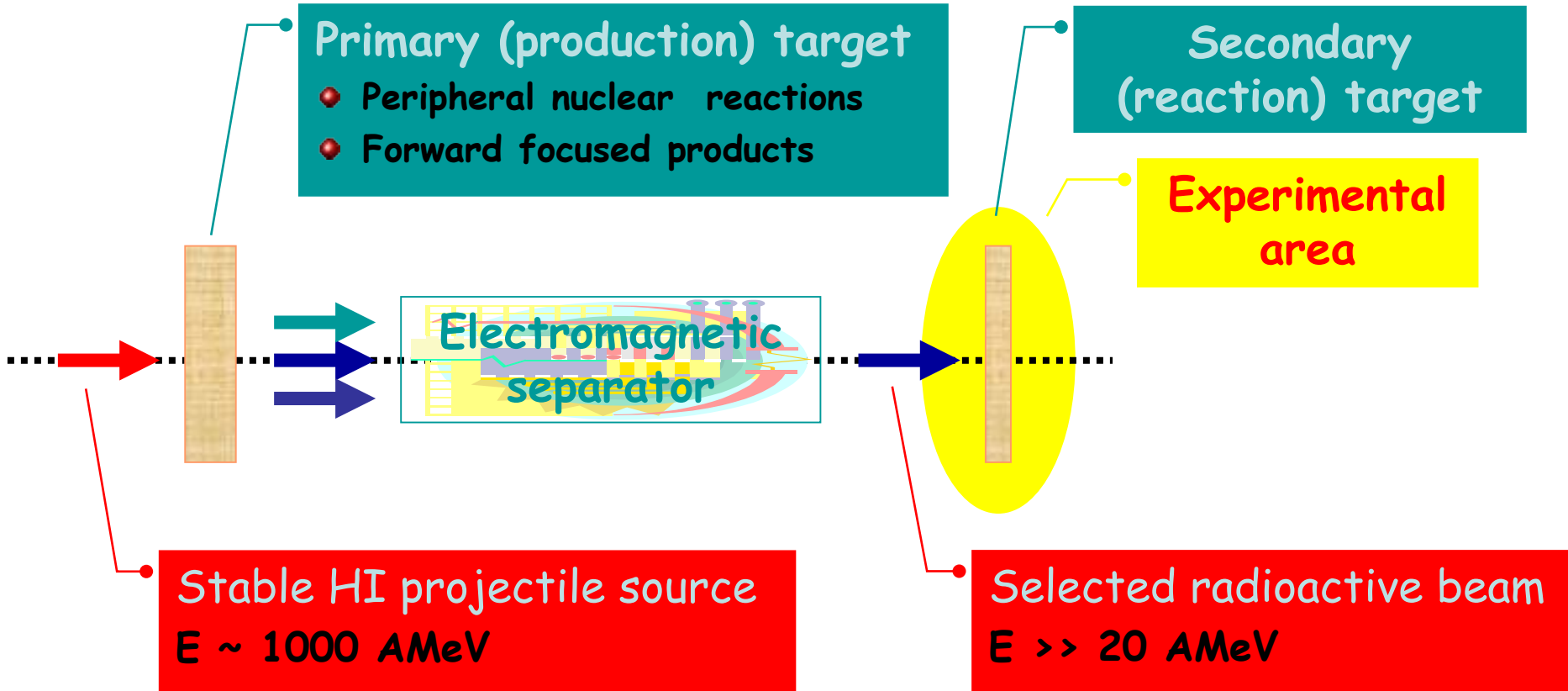
$$\text{with } \mu = \frac{6.02 \cdot 10^{23}}{A_2 [g]} \cdot \sigma_{\text{reaction}} [cm^2]$$

Example: ^{124}Xe on ^9Be \rightarrow ^{104}Sn , $\sigma(^{124}\text{Xe}+^9\text{Be}) = 3.65 [b] \rightarrow \mu_p = 0.244 [cm^2/g]$
 $\sigma(^{104}\text{Sn}+^9\text{Be}) = 3.44 [b] \rightarrow \mu_f = 0.230 [cm^2/g]$

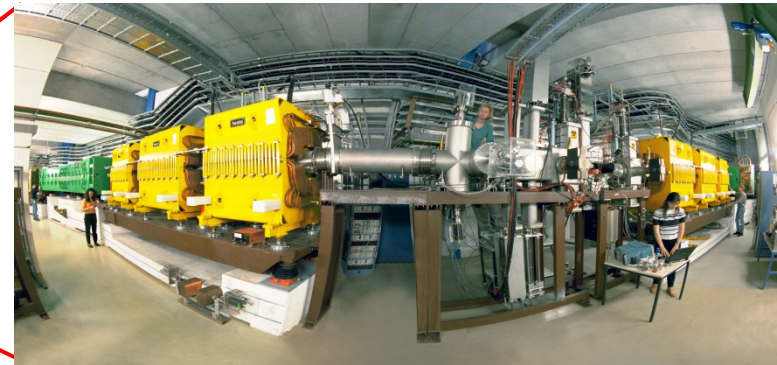
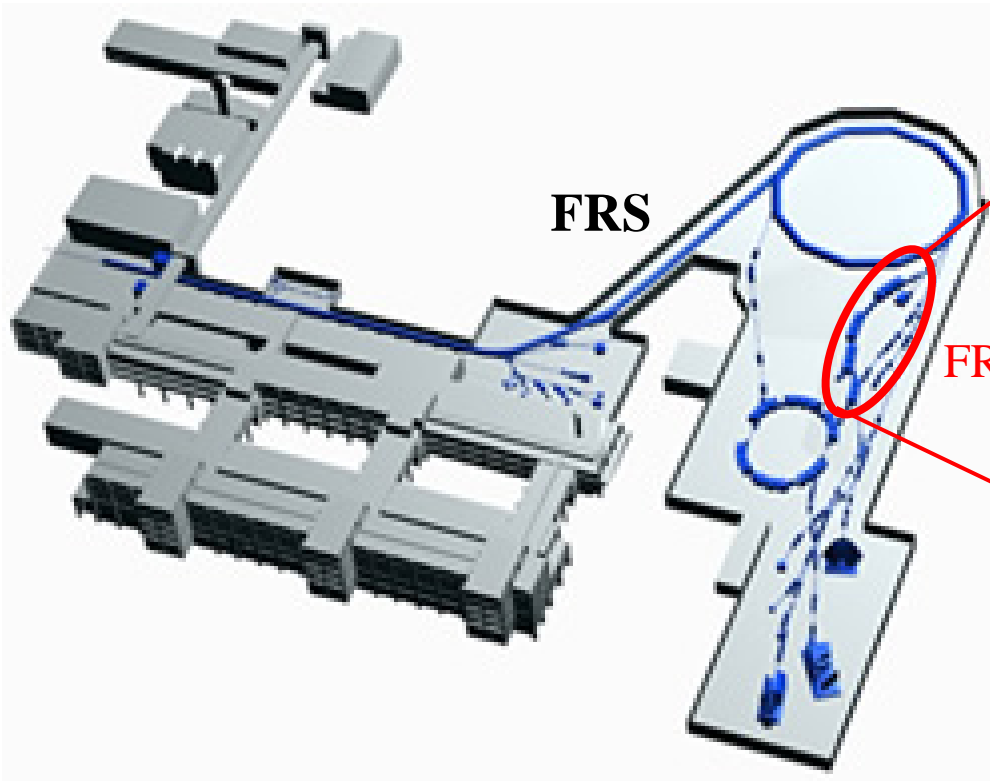
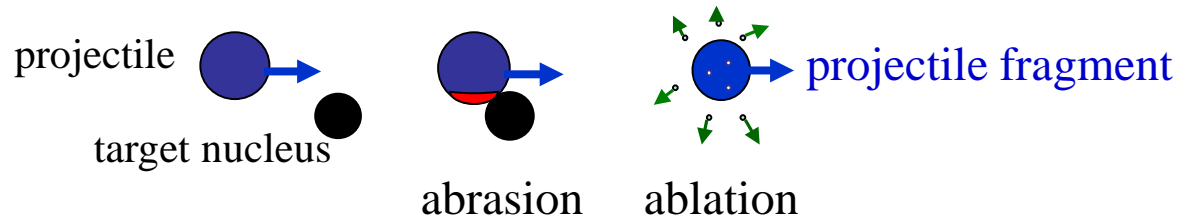


$$\phi_f [s^{-1}] = \phi_p [s^{-1}] - \phi [s^{-1}] = \phi_p [s^{-1}] \cdot \left\{ 1 - e^{-N_t [cm^{-2}] \cdot \sigma_f [cm^2]} \right\} \quad (\text{thick target})$$

In-flight separation of **R**adioactive **I**on **B**eams

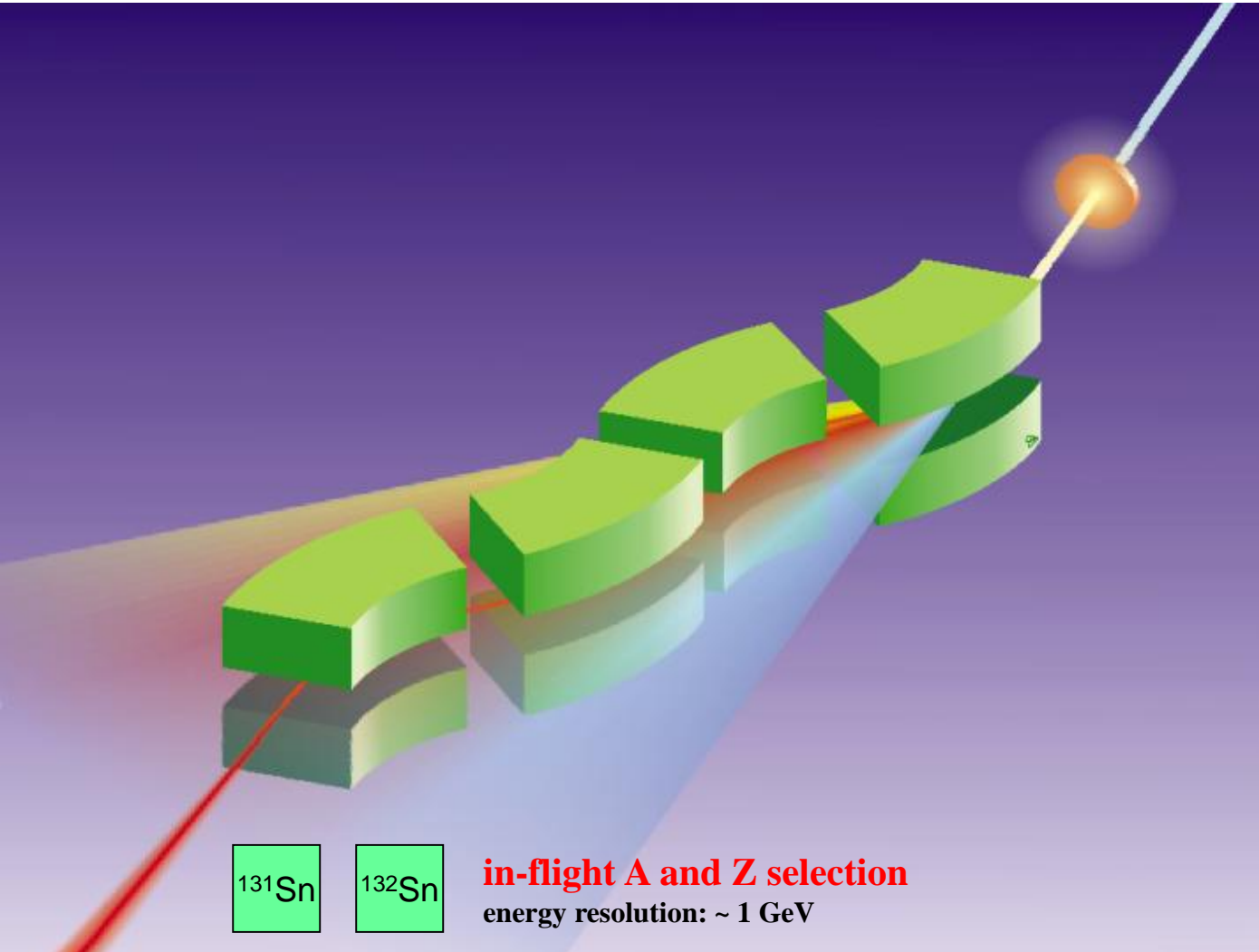


Fragmentation at relativistic energies

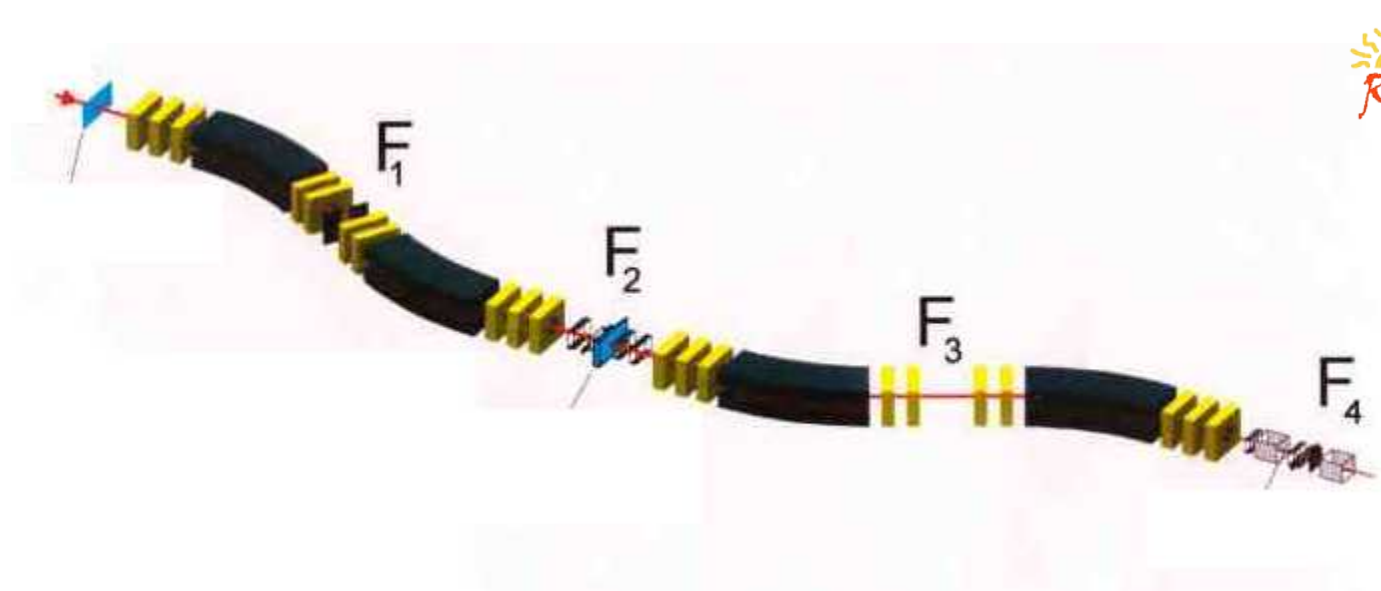
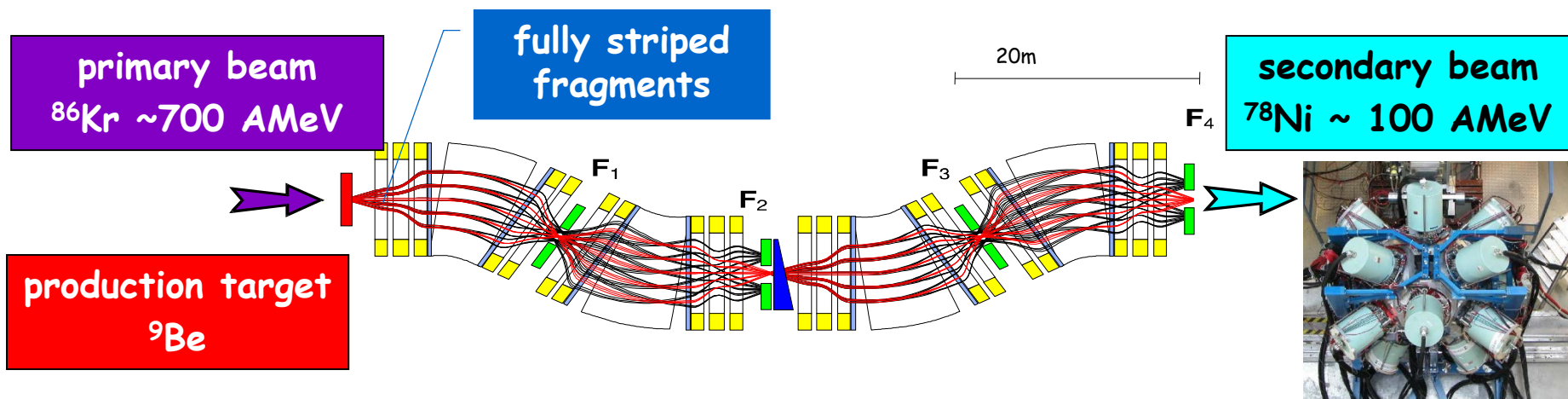


FRagment **S**eparator

FRagment Separator at GSI

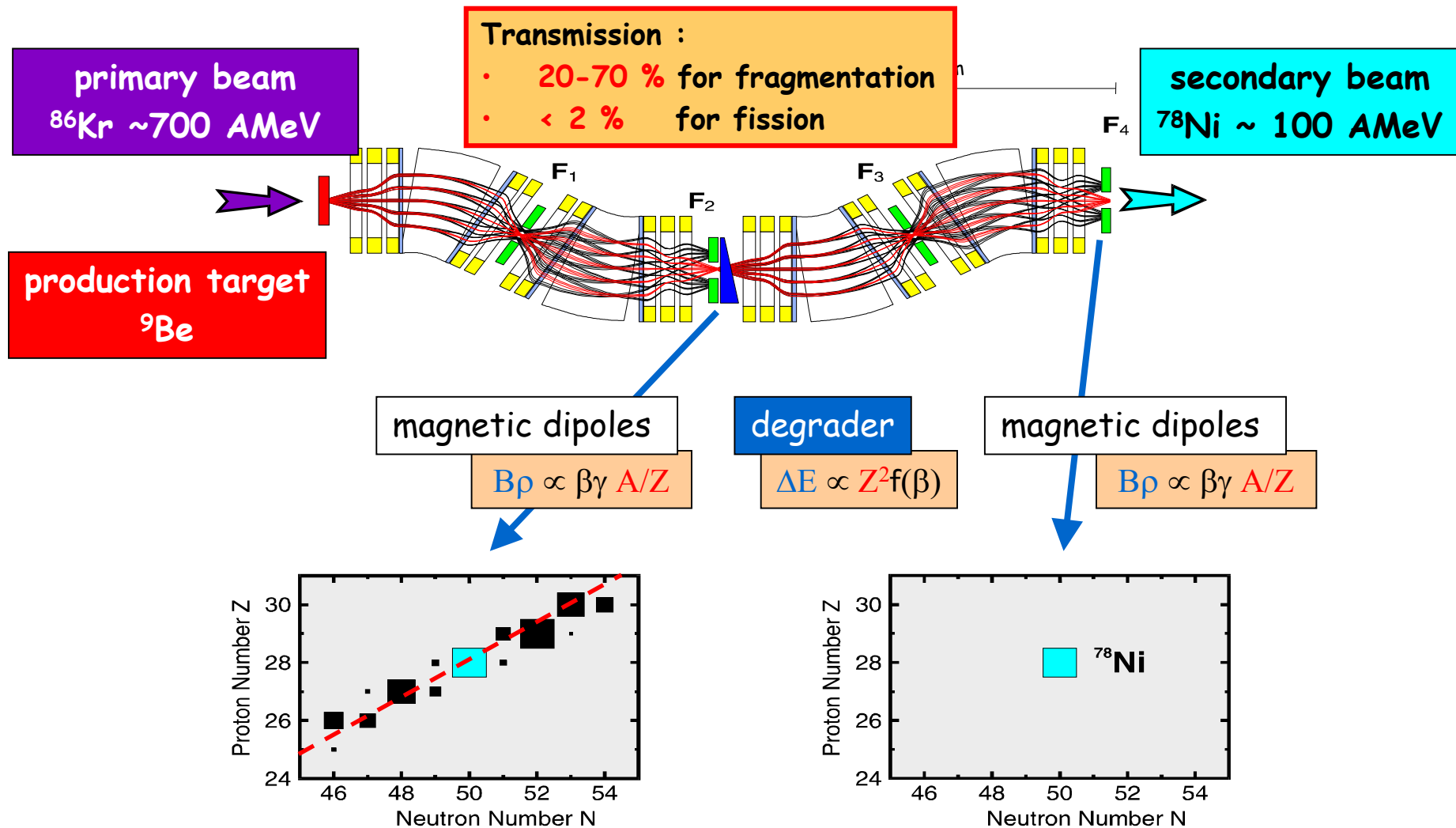


Rare isotope selection at FRS: $B\rho\text{-}\Delta E\text{-}B\rho$ selection

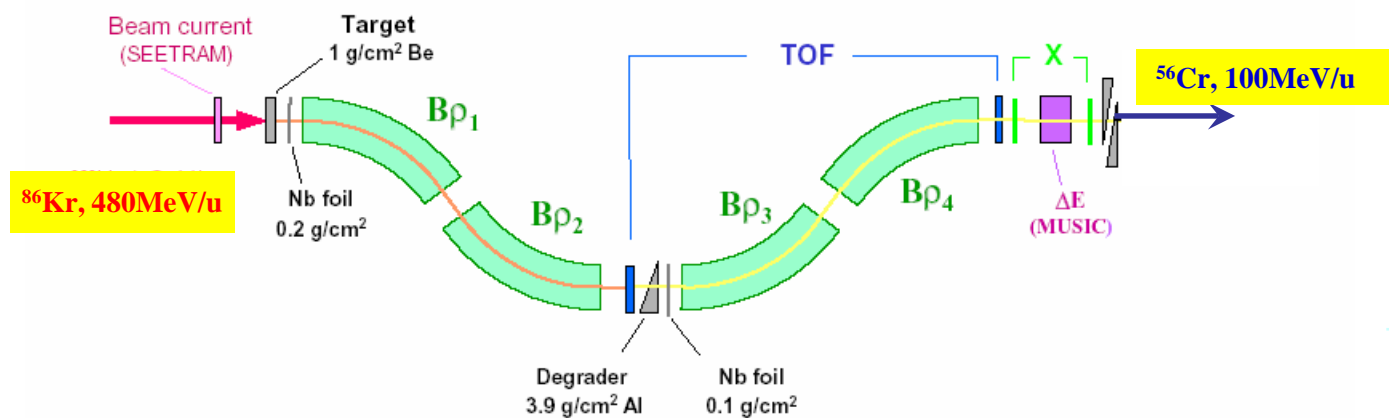
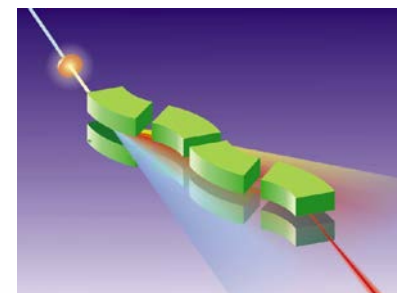
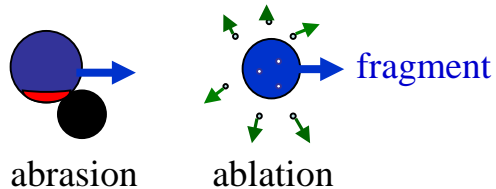
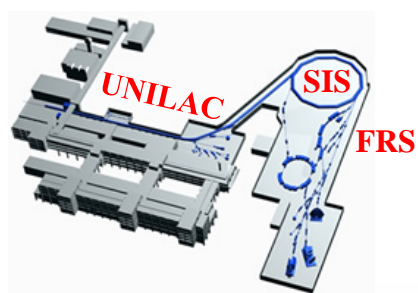


 RISING

Rare isotope selection at FRS: $B\rho$ - ΔE - $B\rho$ selection



Production, separation, identification



Standard FRS detectors



TPC-**x,y**
position
@ S2,S4

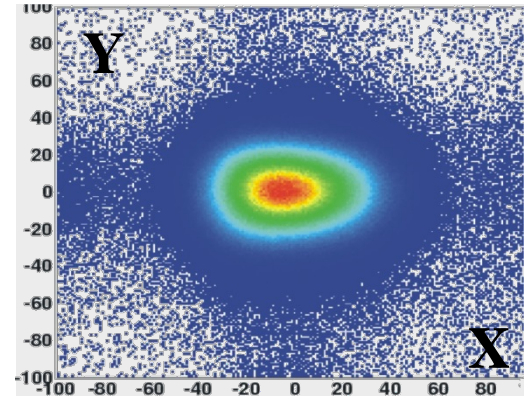
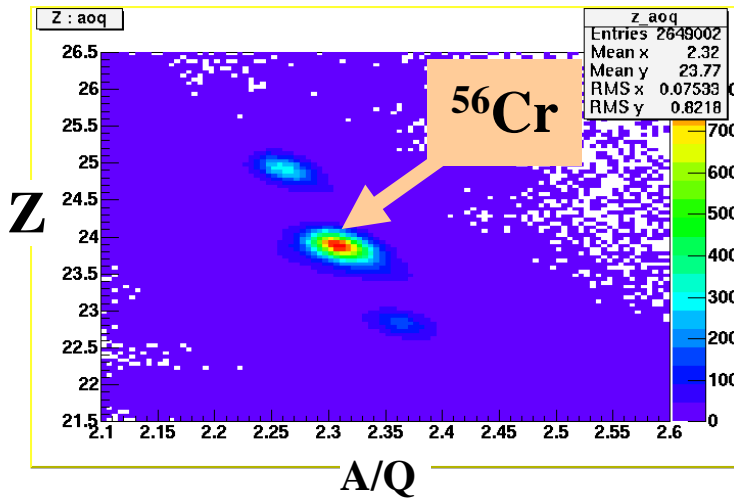
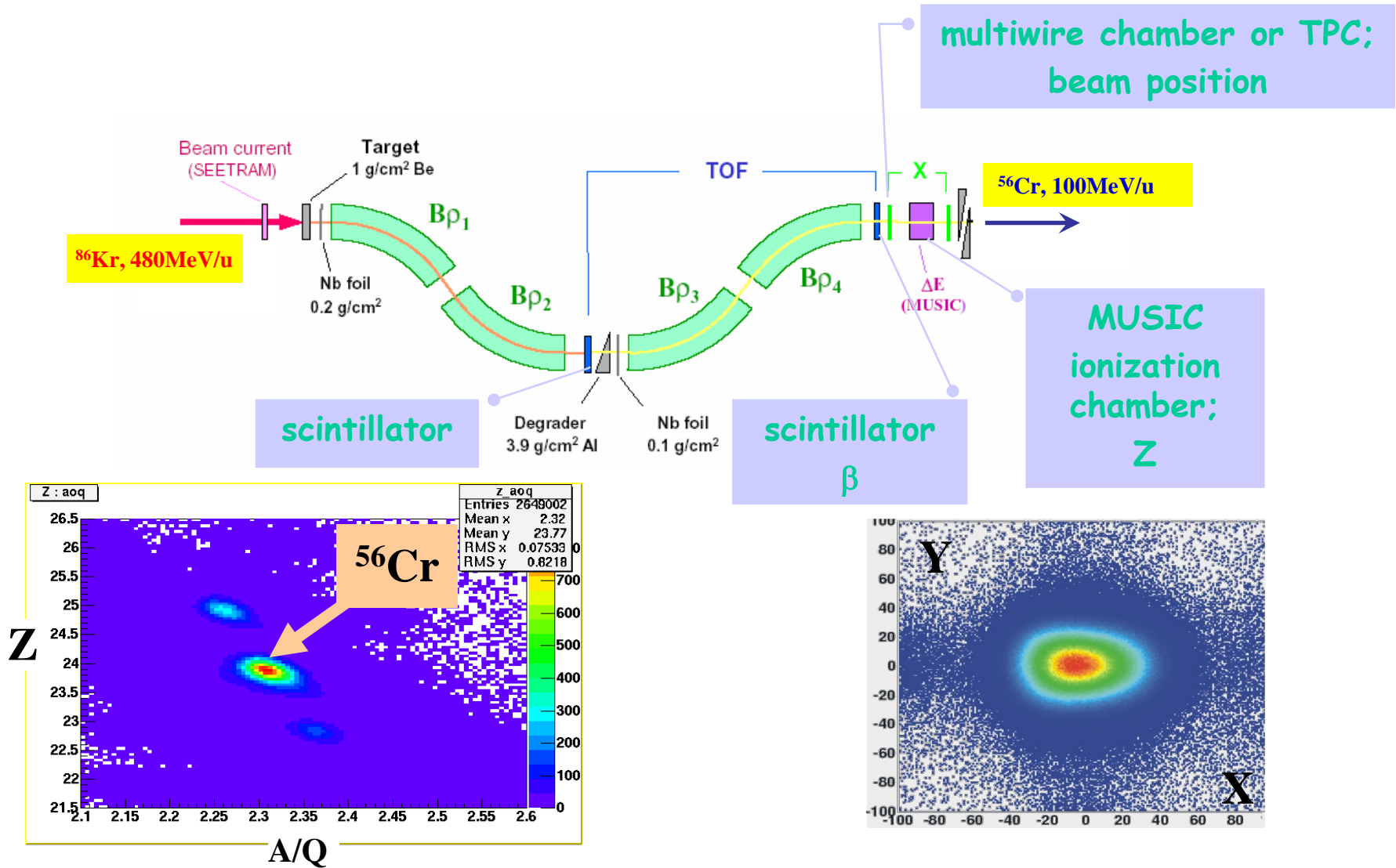


Plastic
scintillator
(**TOF**)
@ S4

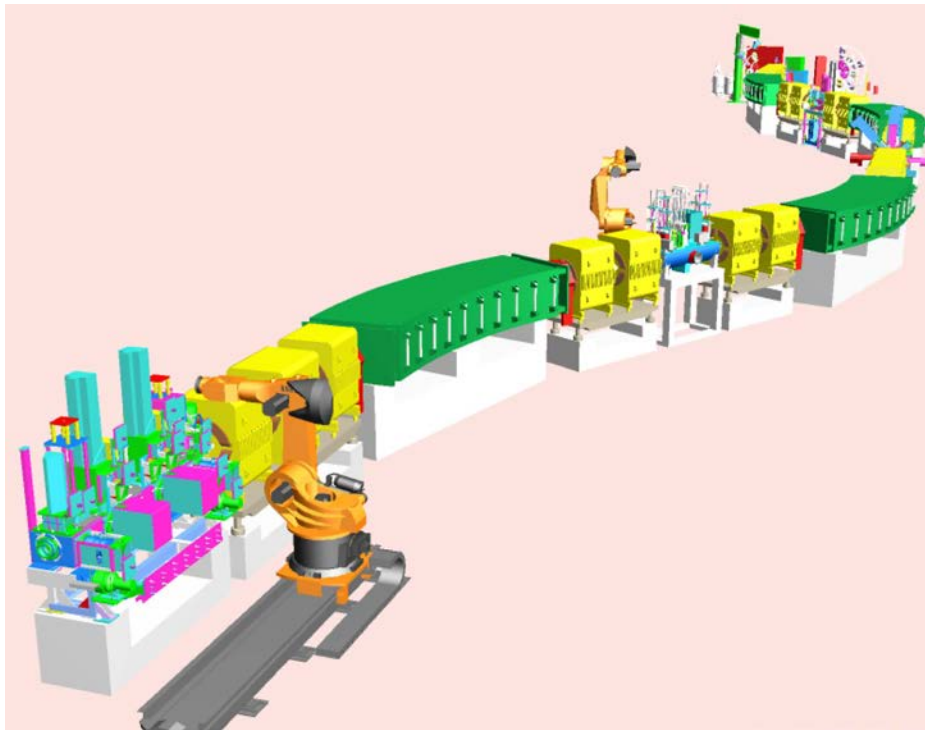
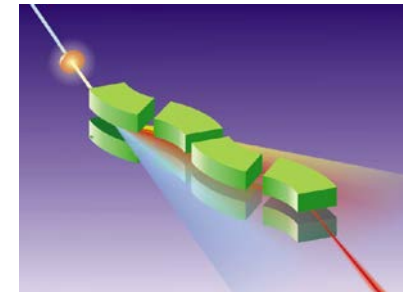
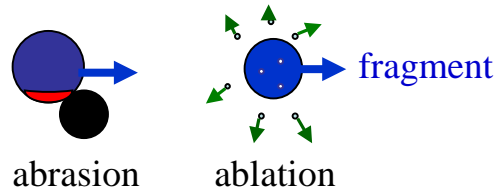
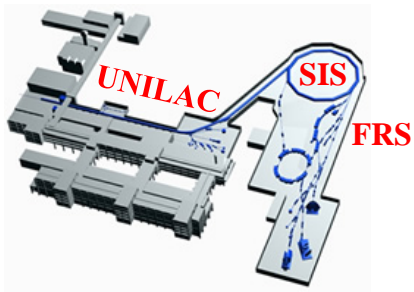


MUSIC
(**ΔE**)
@ S4

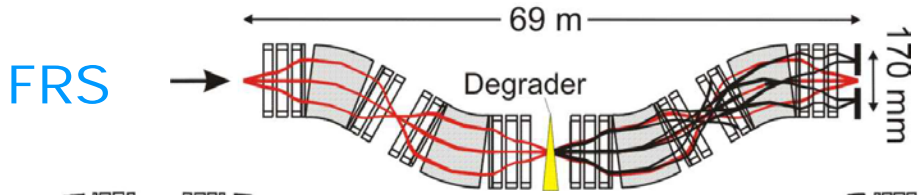
Production, separation, identification



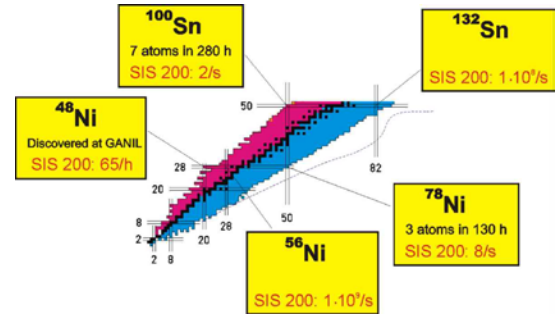
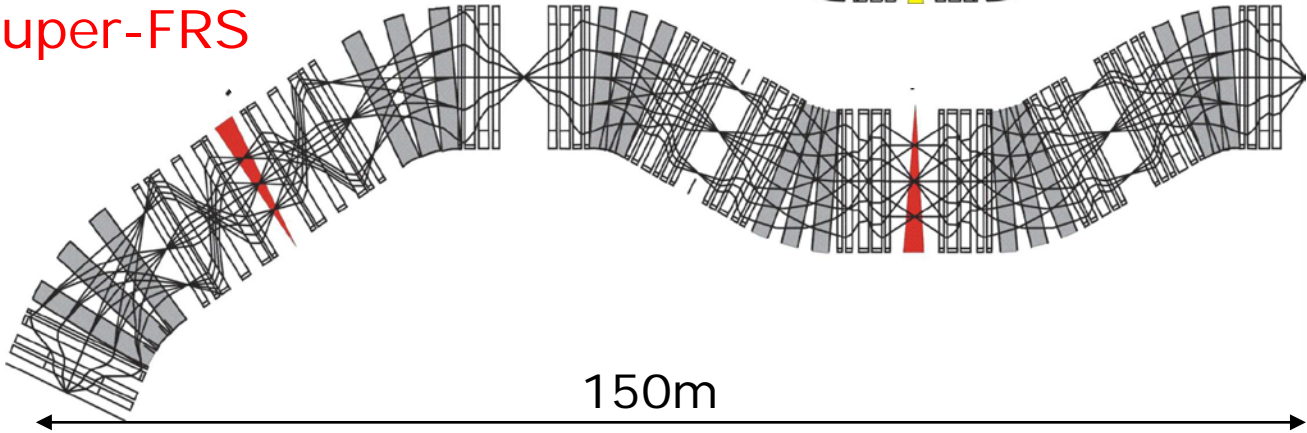
Production, separation, identification



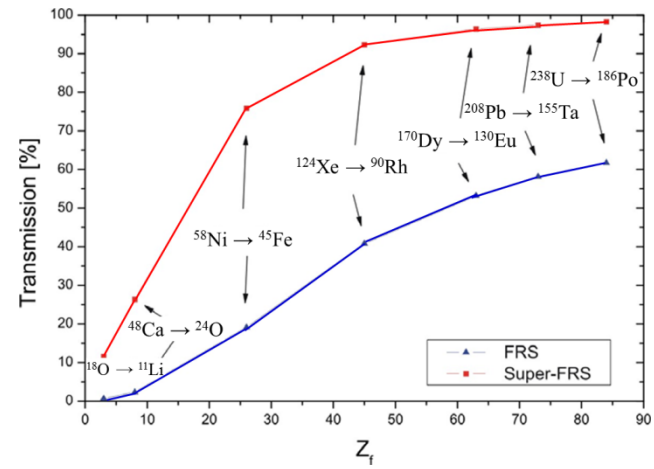
Comparison of FRS with Super-FRS



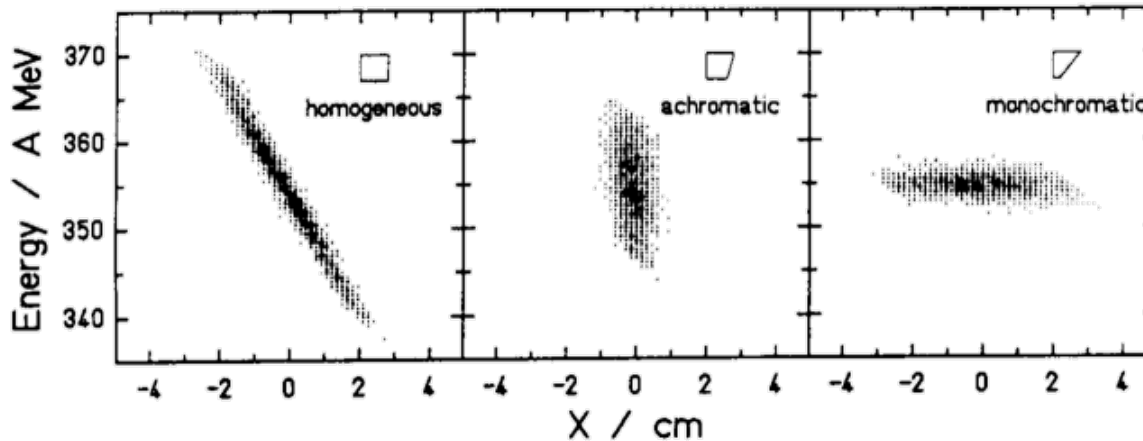
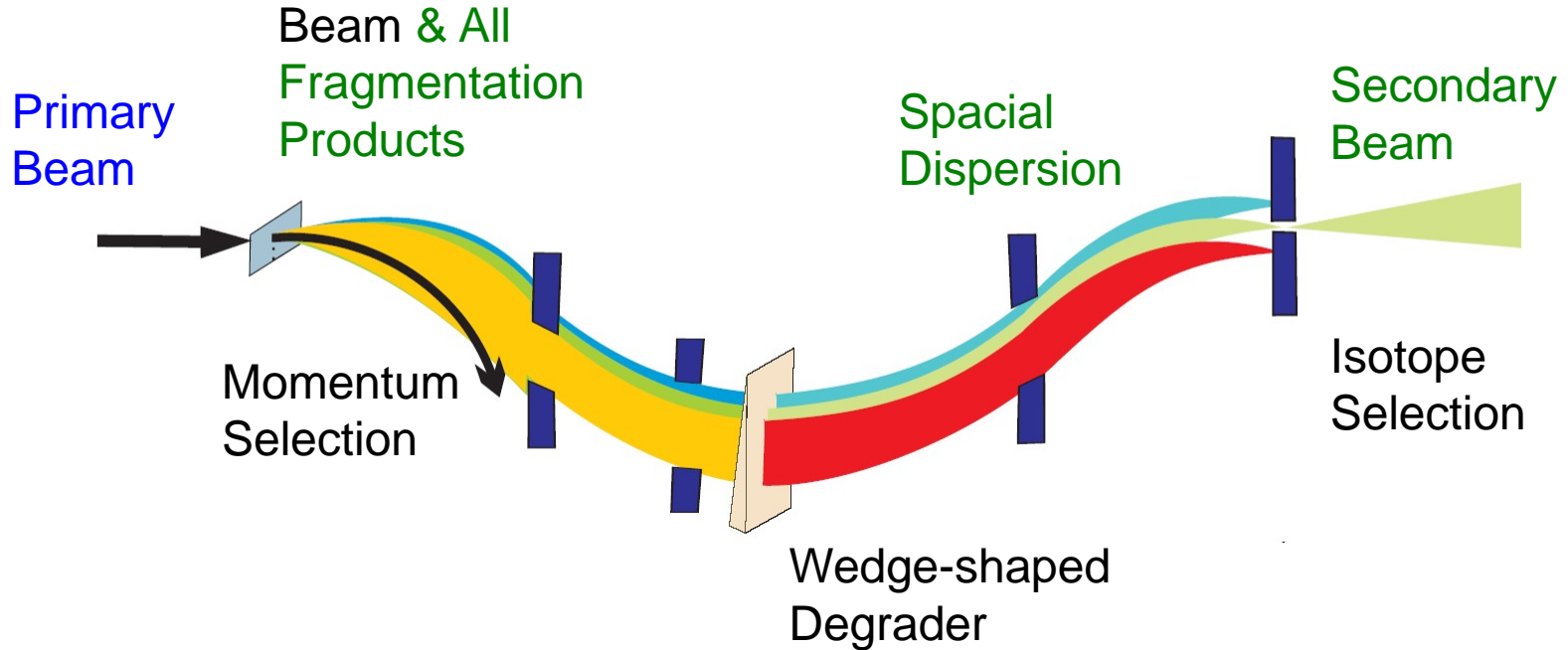
Super-FRS



	$B\rho_{\max}$	$\Delta p/p$	$\Delta\Phi_x, \Delta\Phi_y$	resolving power	gain factor	
					^{19}C	^{132}Sn
FRS	18 Tm	1.0 %	$\pm 13, \pm 13$ mrad	1500	1	1
Super-FRS	20 Tm	2.5 %	$\pm 40, \pm 20$ mrad	1500	5	10
				including primary rate	250	20 000



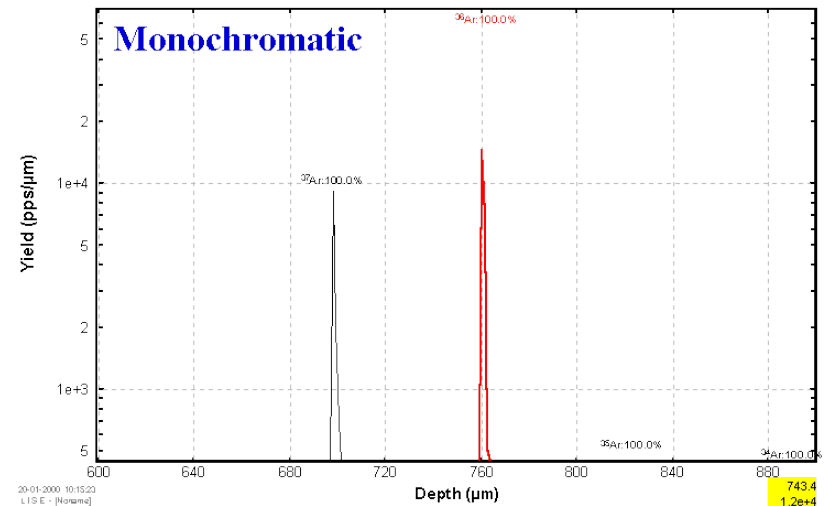
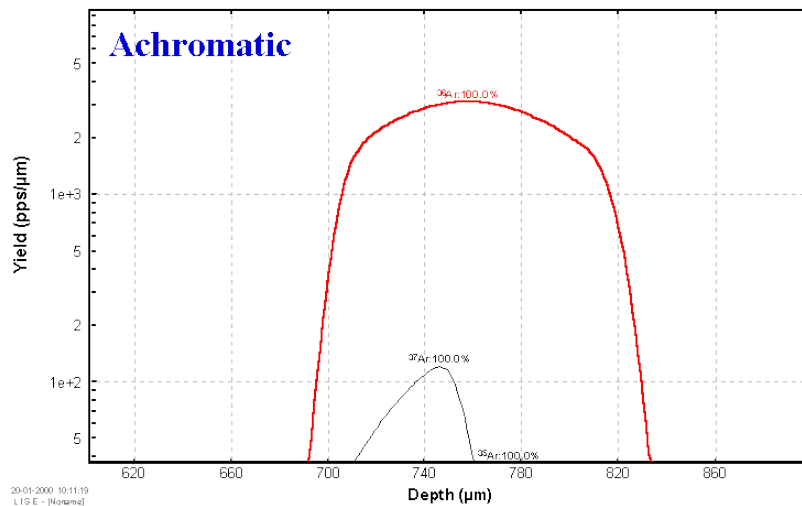
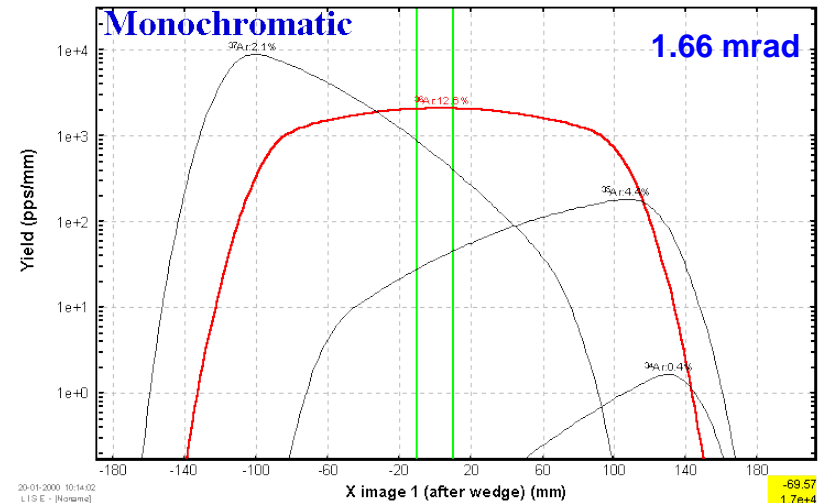
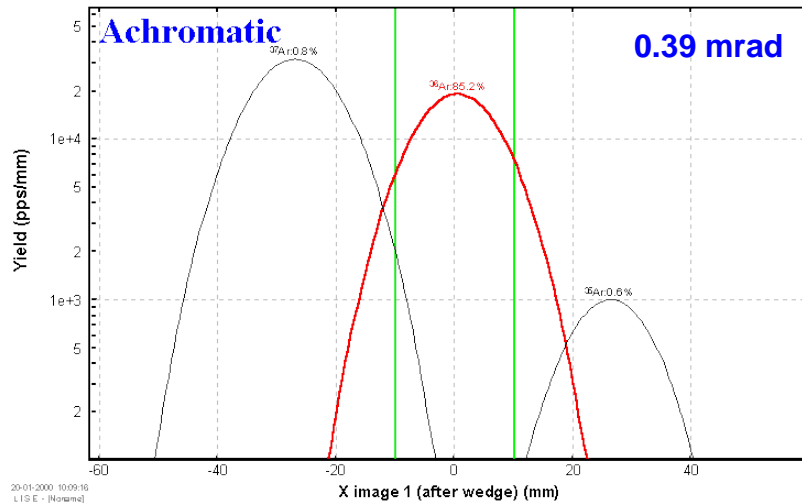
FRagment Separator



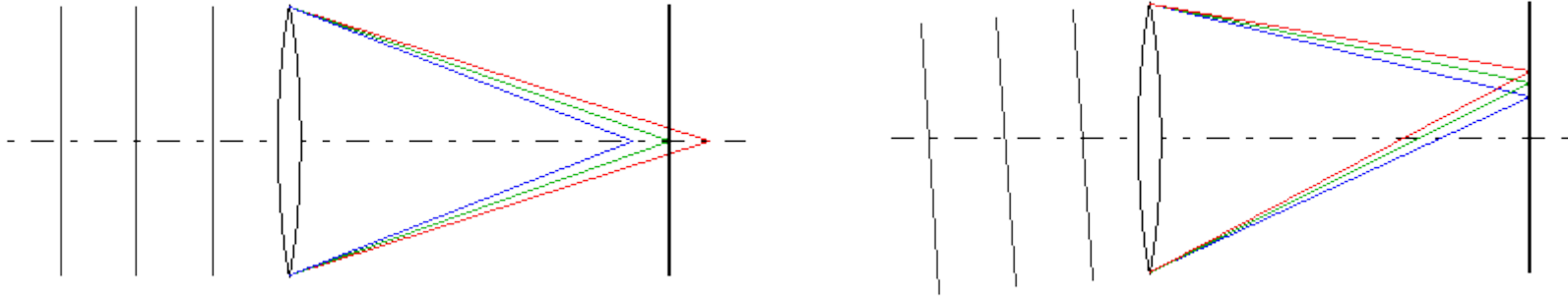
¹⁹Ne at 600A MeV:
Phase-space imaging of differently shaped degraders within the achromatic ion-optical system. The results for a **homogeneous**, an **achromatic**, and a **monoenergetic** degrader are given. All degraders have the same thickness on the optical axis ($d/r=0.5$)

Fragment separation settings

^{40}Ar 50MeV/u + Ta (100 μm), wedge shaped Al (200 μm) degrader



Optics: chromatic aberration



When different **colors** of light propagate at different speeds in a medium, the refractive index is wavelength dependent. This phenomenon is known as **dispersion**.

Longitudinal (axial) chromatic aberration:

The focal planes of the various colors do not coincide.

Transverse (lateral) chromatic aberration:

The size of the image varies from one color to the next.